Radiography 22 (2016) e5–e7

Contents lists available at ScienceDirect

Radiography

journal homepage: www.elsevier.com/locate/radi

Case report

Giant aneurysm of the right internal carotid artery in an 8-month-old child presenting with a persistent red eye

H. Almohiy [a], A. Alamri H [b], C. Saade [a, c, *]

[a] Department of Radiological Sciences, College of Applied Medical Sciences, King Khalid University, Abha, 61431, Saudi Arabia
[b] Department of Ophthalmology, College of Medicine, King Khalid University, Abha, 61421, Saudi Arabia
[c] Department of Diagnostic Radiology, American University of Beirut Medical Center, Lebanon

ARTICLE INFO

Article history:
Received 9 March 2015
Received in revised form
8 June 2015
Accepted 14 June 2015
Available online 30 June 2015

Keywords:
Giant aneurysm
Multidetector computed tomography (MDCT)
Contrast media delivery
Computed tomography angiography

ABSTRACT

Summary: Childhood intracranial aneurysms are a rare entity. Diagnosis of intracranial aneurysms in infancy may be difficult because of their infrequency and confusing clinical presentation. Findings with routine radiographic methods may be misleading and difficult to interpret. This case report entails a giant aneurysm arising from the right internal carotid artery (RICA) in an 8-month-old child.

Introduction

There have been only a handful[1–4] of cases reported in which an arterial aneurysm has been diagnosed during life in an infant under the age of 2 years. Intracranial aneurysms in patients younger than 18 years are reported to account for only 0.005–2% of all diagnosed aneurysms.[5,6] The incidence appears to be particularly low in the neonate (younger than 4 weeks) and infant (younger than 2 years) populations. These are very challenging to diagnose largely due to non-specific clinical presentations. Conventional angiography is the imaging modality of choice[2] with a sensitivity and specificity of 98% and 100% respectively. Nevertheless, MDCT is rapidly approaching the preferred method of imaging in the acute setting with a reported sensitivity and specificity of 90% and 93%.[7,8]

Case report

An 8-month-old male infant presented to the ophthalmology clinic due to red eye, which was persistent for one month. The child was delivered by normal means, spontaneous vaginal delivery after an uncomplicated pregnancy, and the postnatal period was normal. Initial examination in the ophthalmology department revealed an infant with normal light reflex that was steady in both eyes. The portable slit lamp examination demonstrated dilated conjunctival vessels in the right eye. The cornea was clear and fundus examination normal. Intraocular pressure was also normal in both eyes. No signs of trauma were identified. MDCT of the head demonstrated a giant aneurysm originating from the cavernous segment of the ICA. There was no significant dilatation of the circle of Willis arteries (Fig. 1). The patient underwent surgical clipping.

Intracranial MDCT angiogram

The patient was sedated using chloral hydrate which was administered 45 min prior to the CT examination. Chloral hydrate is an appropriate sedation option for non-anesthesiologist physicians due to its low complication rate and high efficacy when used in pediatric patients.[9] Circle of Willis angiogram was performed using a 64-MDCT scanner (VCT Light speed, GE Healthcare; Little Chalfont, UK) with the patient positioned supine with arms by his side. The patient's head was positioned in the isocenter of the scanner with the median sagittal plane and orbitomeatal line (outer canthus of the eye and the center of the external auditory meatus)

* Corresponding author. American University of Beirut, P.O.Box 11-0236, (Department), Riad El-Solh, Beirut 1107 2020 Lebanon.
E-mail addresses: hmohiy@kku.edu.sa (H. Almohiy), amaamri@gmail.com (A. Alamri H), charbel.saade@aub.edu.lb (C. Saade).

http://dx.doi.org/10.1016/j.radi.2015.06.002
1078-8174/

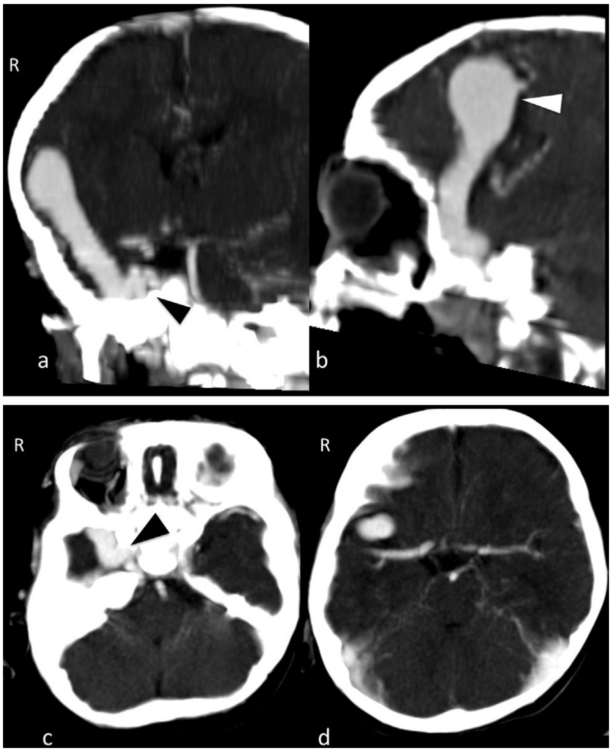

Figure 1. (a) coronal maximum intensity projection of the giant aneurysm at the level of the clivus originating from the cavernous segment (black arrow head) of the internal carotid artery, (b) sagittal maximum intensity projection of the giant aneurysm (white arrow head) parallel to the long axis of the aneurysm in the partotemporal region demonstrating the extent of growth within the cranium, (c and d) axial maximum intensity projection of the giant aneurysm at the level of the pituitary fossa (c) and above the roof of cranium (d) which is clearly displaced from the right middle cerebellar artery.

adjusted to be perpendicular to the table top. Anterior-posterior and lateral scout scans were performed, with a scan range from the apex of the cranial vault to the base of skull (2 cm below). The scan parameters were: detector width 64 × 0.625 mm; pitch 0.984:1; rotation time 0.4 s; exposure factors 80 kVp, 150 mA, with z-axis modulation; scanning time of 1.6 s. Image Reconstruction parameters were set: standard filtered back projection reconstruction of axial images at 0.625 mm slice width, reconstruction interval of 0.5 mm, field of view of 350 × 350 mm with a window width and level of 350 and 50 respectively. A craniocaudal scan direction was employed.

Contrast bolus geometry

Bolus geometry is the pattern of enhancement, measured in a region of interest (ROI), plotted on a time(s)/attenuation HU (Hounsfield units) curve, after intravascular injection of contrast material. A test bolus technique was employed to determine three ROI's (Region Of Interest) that were plotted inside the circle of Willis (right and left middle cerebellar and basilar arteries), with a small amount of contrast material (1 ml) introduced at the same rate as the main bolus when injected using the Optibolus technique. This ROI assessed the time to peak (TTP) and determined the arteriovenous circulation time for intracranial vasculature (Fig. 2).

Contrast medium administration

Contrast material was injected with an automated dual barrel power injector (Optivantage, Covidien, Cincinnati) via a 24 gauge venous catheter in the right arm. The right antecubital vein was used in this study because it provides the shortest path for the contrast material to pass through the venous system with the least amount of dilution, promoting good image quality during computed tomography angiography (CTA).[8,10–13] The contrast media volume was predetermined by employing a 2:1 contrast per ml per kg. The patient was 7 kg which equated to 14 ml of contrast volume (Ioversol, 370 mg per ml iodine Optiray, Mallinckrodt, Cincinnati), followed by a 15 ml saline chaser. Both contrast media and saline chaser were injected at a flow rate of 2.2 ml/s.

Management

The patient underwent coordinated procedures, commencing with a right intraoperative aneurysmal clipping from RICA. The

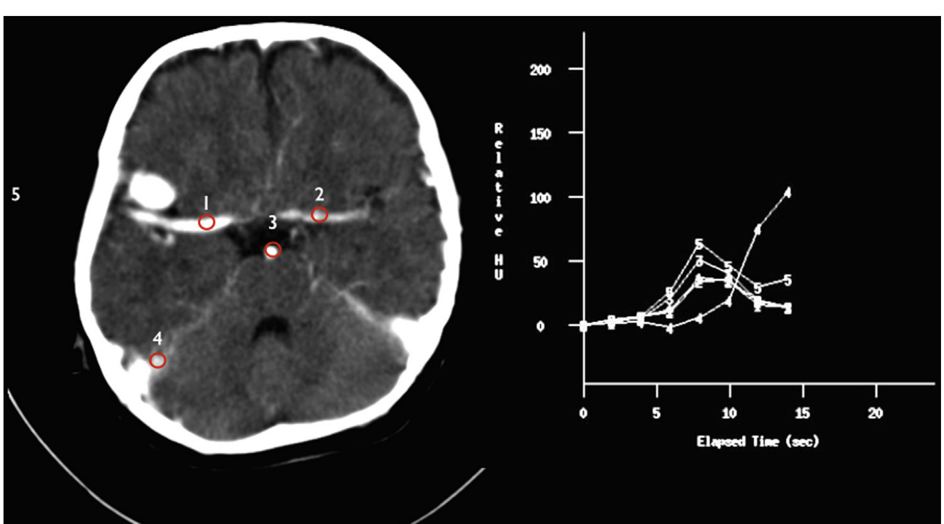

Figure 2. Demonstrates the timing bolus is used to determine the TTP of the intracranial vessels. The axial head CT image demonstrates the four ROIs measured. ROI's 1–3 measured the intracranial circulation and ROI 4 (draining arterial supply from the right side of the brain) and therefore, in this case study the scanner acquisition started at peak arterial opacification in the aneurysm and just prior to the venous circulation.

other surrounding vessels such as M1, M2 and M3 branches of the middle cerebral artery (MCA) had no associated aneurysms. A repeat cerebral angiography was performed, demonstrating successful clipping of the aneurysm. After surgical intervention the patient improved dramatically with resolution of his dilated, tortuous conjunctival blood vessles, his slit lamp examination showed normal anterior segment examination, funduscopy was normal. The patient's post-operative course was unremarkable. He was discharged on postoperative day five. Microscopic examination showed that the aneurysm was a true arterial one. The patient was seen 6 months later and his condition was unremarkable.

Discussion

Neonates and infants often present with nonspecific signs such as irritability, seizures, drowsiness, or emesis. Whilst childhood aneurysms are infrequent, the most common site is encountered at the carotid apex and the vertebrobasilar system. Large (>1 cm) or giant (>2.5 cm) aneurysms are more common in children and are associated with mass effect and seizures.

Contrast medium administration and parameters affecting bolus geometry need to be carefully configured to match the arterial and venous enhancement pattern of intracranial aneurysms during MDCT.[14–16] Identification of the recruited feeding vessels from the adjacent normal arteries following occlusion of the arterial supply and drainage of venous structures should be determined prior to intervention.

Management options include transarterial and transvenous embolization, ligation of feeding vessels, injection of sclerosant into the lesion and surgical excision.[17–19] In our case, owing to the significant size of the aneurysm, the patient underwent surgical clipping.

Conclusion

Evaluation of the angioarchitecture in giant aneurysms in the intracranial vault is considerably improved with the use of MDCT angiography.

Conflict of interest

None.

References

1. Abla AA, Zaidi HA, Crowley RW, Britz GW, McDougall CG, Albuquerque FC, et al. Optic chiasm compression from mass effect and thrombus formation following unsuccessful treatment of a giant supraclinoid ICA aneurysm with the pipeline device: open surgical bailout with STA-MCA bypass and parent vessel occlusion. *J Neurosurg Pediatr* 2014;**14**(1):31–7.
2. Gemmete JJ, Toma AK, Davagnanam I, Robertson F, Brew S. Pediatric cerebral aneurysms. *Neuroimaging Clin N Am* 2013;**23**(4):771–9.
3. Alurkar A, Karanamm LS, Oak S. Role of endovascular treatment in pediatric cerebral aneurysms: a series of two case reports. *J Clin Imaging Sci* 2012;**2**:75.
4. Proust F, Toussaint P, Garnieri J, Hannequin D, Legars D, Houtteville JP, et al. Pediatric cerebral aneurysms. *J Neurosurg* 2001;**94**(5):733–9.
5. Suarez JI. Treatment of ruptured cerebral aneurysms and vasospasm after subarachnoid hemorrhage. *Neurosurg Clin N Am* 2006;**17**(Suppl. 1):57–69.
6. Molyneux AJ. Ruptured intracranial aneurysms - clinical aspects of subarachnoid hemorrhage management and the international subarachnoid Aneurysm trial. *Neuroimaging Clin N Am* 2006;**16**(3):391–6. vii-viii.
7. Jayaraman MV, Mayo-Smith WW, Tung GA, Haas RA, Rogg JM, Mehta NR, et al. Detection of intracranial aneurysms: multi-detector row CT angiography compared with DSA. *Radiology* 2004;**230**(2):510–8.
8. Saade C, Bourne R, Wilkinson M, Evanoff M, Brennan P. A reduced contrast volume acquisition regimen based on cardiovascular dynamics improves visualisation of head and neck vasculature with carotid MDCT angiography. *Eur J Radiol* 2013;**82**(2):e64–9.
9. Delgado J, Toro R, Rascovsky S, Arango A, Angel GJ, Calvo V, et al. Chloral hydrate in pediatric magnetic resonance imaging: evaluation of a 10-year sedation experience administered by radiologists. *Pediatr Radiol* 2015;**45**(1):108–14.
10. de Monye C, Cademartiri F, de Weert TT, Siepman DA, Dippel DW, van Der Lugt A. Sixteen-detector row CT angiography of carotid arteries: comparison of different volumes of contrast material with and without a bolus chaser. *Radiology* 2005;**237**(2):555–62.
11. You SY, Yoon DY, Choi CS, Chang SK, Yun EJ, Seo YL, et al. Effects of right- versus left-arm injections of contrast material on computed tomography of the head and neck. *J Comput Assist Tomogr* 2007;**31**(5):677–81.
12. Saade C, Bourne R, Wilkinson M, Evanoff M, Brennan PC. Caudocranial scan direction and patient-specific injection protocols optimize ECG-gated and non-gated thoracic CTA. *J Comput Assist Tomogr* 2013;**37**(5):725–31.
13. Saade C, Bourne R, El-Merhi F, Somanathan A, Chakraborty D, Brennan P. An optimised patient-specific approach to administration of contrast agent for CT pulmonary angiography. *Eur Radiol* 2013;**23**(11):3205–12.
14. Saade C, Bourne R, Wilkinson M, Brennan P. Contrast Medium Administration and Parameters Affecting Bolus geometry in multidetector computed tomography angiography: an overview. *J Med Imaging Radiat Sci* 2011;**42**(3):113–7.
15. Saade C, Wilkinson M, Parker G, Dubenec S, Brennan P. Multidetector computed tomography in the evaluation of cirsoid aneurysm of the scalp—a manifestation of trauma. *Clin Imaging* 2013;**37**(3):558–60.
16. Saade C, Bourne R, Wilkinson M, Brennan PC. MDCT angiography of the major congenital anomalies of the extracranial arteries: pictorial review. *J Med Imaging Radiat Oncol* 2013;**57**(3):321–8.
17. Gurkanlar D, Gonul M, Solmaz I, Gonul E. Cirsoid aneurysms of the scalp. *Neurosurg Rev* 2006;**29**(3):208–12.
18. Hage ZA, Few JW, Surdell DL, Adel JG, Batjer HH, Bendok BR. Modern endovascular and aesthetic surgery techniques to treat arteriovenous malformations of the scalp: case illustration. *Surg Neurol* 2008;**70**(2):198–203 [discussion].
19. Shenoy SN, Raja A. Scalp arteriovenous malformations. *Neurol India* 2004;**52**(4):478–81.